Thermal photon production in high-energy nuclear collisions

John J. Neumann,* David Seibert,† and George Fai‡

Center for Nuclear Research, Department of Physics, Kent State University, Kent, Ohio 44242

(Received 12 September 1994)

We use a boost-invariant one-dimensional (cylindrically symmetric) fluid dynamics code to calculate thermal photon production in the central rapidity region of S+Au and Pb+Pb collisions at SPS energy ($\sqrt{s} = 20$ GeV/nucleon). We assume that the hot matter is in thermal equilibrium throughout the expansion, but consider deviations from chemical equilibrium in the high-temperature (deconfined) phase. We use equations of state with a first-order phase transition between a massless pion gas and quark gluon plasma, with transition temperatures in the range $150 \leq T_c \leq 200$ MeV.

PACS number(s): 25.75.+r, 24.85.+p, 13.85.Qk

I. INTRODUCTION

Electromagnetic probes (photons and leptons) have long mean free paths in hadronic matter and are therefore well suited for studying the earliest stages of ultrarelativistic nuclear collisions. Preliminary single photon spectra from 200 GeV/nucleon S+Au collisions at CERN's Super Proton Synchrotron (SPS) have recently become available from the WA80 experiment [1], and results from Pb+Pb collisions should be available in the near future. In the present work we calculate thermal photon spectra in the central rapidity region for SPS collisions, based on a boost-invariant fluid-dynamical description of the hot matter; a similar approach was used in Ref. [2].

Earlier predictions of photon spectra [3] and of dileptons from several resonances [4–6] show a useful sensitivity to the assumed QCD transition temperature when the equation of state incorporates a strong first-order phase transition and transverse expansion is neglected. The correlation between the apparent temperatures of photon spectra and the assumed transition temperature was suggested as a thermometer for the transition temperature [3]. One question we wish to study here is whether a useful correlation can still be found if transverse expansion is taken into account.

In our calculation we assume a boost-invariant longitudinal expansion as discussed by Bjorken [7], coupled to a cylindrically symmetric transverse expansion. The one-dimensional fluid dynamics code we developed uses the Godunov method as described by Blaizot and Ollitrault [8]. We assume thermal equilibrium throughout the evolution of the system, but consider deviations from chemical equilibrium in the high-temperature phase by allowing the quark and antiquark densities to be a (fixed) frac-

tion of the equilibrium value. In the photon production rate we include the effect of the a_1 resonance. We calculate the transverse momentum distribution for photons in the range $1 \leq p_T \leq 2$ GeV. We investigate the sensitivity to different assumptions about the initial temperature, freeze-out temperature, and quark fraction, and compare production rates to the preliminary WA80 data. We use standard high-energy conventions, $c = \hbar = k_B = 1$.

II. FLUID-DYNAMICAL EVOLUTION

For high collision energy we expect longitudinal boost invariance [7], so the behavior of the produced matter at different rapidities is the same in the longitudinally comoving frame for fixed proper time $\tau = \sqrt{t^2 - z^2}$, where z is the distance along the beam axis. At $\tau = 0$ the colliding nuclei reach the point of maximum overlap and are assumed to form a longitudinally expanding pancake. The hot matter has thermalized at $\tau = \tau_0$ (≈ 0.2 fm/c [9,10]), when transverse expansion begins, coupled to the longitudinal expansion. We treat the hot matter as one dimensional, assuming cylindrical symmetry and boost invariance with equations of motion [8]

$$\frac{\partial}{\partial \tau}(r\tau T^{00}) + \frac{\partial}{\partial r}(r\tau T^{r0}) = -rP, \tag{1a}$$

$$\frac{\partial}{\partial \tau}(r\tau T^{0r}) + \frac{\partial}{\partial r}(r\tau T^{rr}) = \tau P. \tag{1b}$$

Here P is the pressure, r is the radial coordinate, and the energy-momentum tensor $T^{\mu\nu}$ is $T^{\mu\nu} = (e + P)u^\mu u^\nu - P g^{\mu\nu}$, with e being the energy density, u the four-velocity, and metric tensor $g^{\mu\nu} = \text{diag}(1, -1, -1, -1)$. The r weighting takes into account the radial geometry, and the τ dependence is due to the coupling between the longitudinal and transverse expansions.

The fluid dynamics code uses the Godunov method as described by Blaizot and Ollitrault [8]. The system is described by the relativistically covariant energy-momentum tensor elements T^{00} and T^{0r}. The program calculates the changes in the cell averages of these tensor elements, respectively Θ^{00} and Θ^{0r}, by calculating the

*Electronic address (internet): neumann@scorpio.kent.edu

†Current address: Department of Physics, McGill University, 3600 University St., Montreal, QC, H3A 2T8, Canada. Electronic address (internet): seibert@hep.physics.mcgill.ca

‡Electronic address (internet): fai@ksuvxd.kent.edu

flows T^{0r} and T^{rr} across the cell walls. A relationship between the flows at the walls and the changes in $\Theta^{\mu\nu}$ is found by integrating (1) over each space-time cell, assuming plane similarity forms for the flow patterns. We approximate the space-time averaged pressure $\langle P \rangle$ by using the initial value of $T^{\mu\nu}$ to estimate $\Theta^{\mu\nu}$ at intermediate times, and constructing $\langle P \rangle$ from these estimates for Θ^{00} and Θ^{0r}. This estimated value of $\langle P \rangle$ is then used to solve for $\Theta^{\mu\nu}$ at the end of the time step. At the beginning of the next time step, we set T^{00} and T^{0r} throughout each cell equal to Θ^{00} and Θ^{0r} for that cell at the end of the previous step.

From $\tau = 0$ until the transverse expansion starts at $\tau = \tau_0$, we assume a boost-invariant cylinder of radius $R_<$ (the radius of the smaller nucleus), filled uniformly with quark gluon plasma (QGP) at temperature $T = T_0$. This is approximately compatible with the initial entropy density for short times [11]. We determine T_0 by assuming entropy conservation for $\tau > \tau_0$; hence

$$s(T_0) = \frac{3.6\, dN/dy}{\pi\, R_<^2\, \tau_0},\tag{2}$$

where s is the entropy density, with total (charged plus neutral) multiplicity density $dN/dy = 240$ and 1600 for S+Au and Pb+Pb collisions, respectively.

The equations of state (EOS's) that we use here are of the form

$$T < T_c: \quad \begin{cases} e = \dfrac{\pi^2}{10} T^4, \\[2mm] P = \dfrac{e}{3}, \end{cases}\tag{3a}$$

$$T = T_c: \quad \begin{cases} \dfrac{\pi^2}{10} T_c^4 \le e \le \dfrac{\pi^2}{30} g_q T_c^4 + B, \\[2mm] \dfrac{\pi^2}{30} T_c^4 = P = \dfrac{\pi^2}{90} g_q T_c^4 - B, \end{cases}\tag{3b}$$

$$T > T_c: \quad \begin{cases} e = \dfrac{\pi^2}{30} g_q T^4 + B, \\[2mm] P = \dfrac{\pi^2}{90} g_q T^4 - B, \end{cases}\tag{3c}$$

where g_q is the number of massless degrees of freedom in the deconfined phase. We treat only the case of zero baryon density, so the entropy density is

$$s = \frac{e + P}{T},\tag{4}$$

independent of the phase of the matter. Below T_c, the EOS is that of a massless pion gas. Because recent calculations have predicted that the quarks may reach only a fraction of their equilibrium number by the beginning of transverse expansion [9,10], we take $g_q = 16 + 21x$, where x is a parameter that we vary between 0 and 1 to simulate the effect of reducing the quark density in the QGP below the equilibrium value (x=1 is equilibrium for two flavors of massless quarks). The vacuum energy density in the deconfined phase, B, is related to the transition temperature T_c by requiring equal pressures in the deconfined and hadronic phases at $T = T_c$:

$$B = \frac{\pi^2 (g_q - 3)}{90} T_c^4.\tag{5}$$

For all the fluid dynamic calculations we have taken the radial cell size δr and time step $\delta\tau$ small enough to be within a few percent of the continuum limit. We also required $\delta\tau \ll \delta r/2$, guaranteeing that a similarity pattern from one side of a cell does not overlap the opposite side of the cell or the pattern from the other side. Also, because the radial pattern size is much smaller than δr, we may assume plane similarity solutions as a good approximation of the intercell flow in spite of the radial geometry of the system.

III. THERMAL PHOTONS

The central region photon p_T distribution from boost-invariant hot matter is

$$\left.\frac{d^2 N_\gamma}{p_T\, dp_T\, dy}\right|_{y=0} = \int d\eta \int d\tau\, \tau \int dr\, 2\pi r \int_0^\pi d\theta\, \sin\theta \int_0^{2\pi} d\phi \int_0^\infty dp\, p^2\, \frac{dR}{d^3 p}$$

$$\times \delta\left(\frac{1}{2} p_T^2 - \frac{1}{2} p_T'^2\right) \delta\left[\eta + \tanh^{-1}\left(\frac{\cos\theta}{\gamma\, |1 + v\sin\theta\cos\phi|}\right)\right],\tag{6}$$

where

$$p_T'^2 = p^2 \gamma^2 [\sin^2\theta + 2v\sin\theta\cos\phi + v^2 (1 - \sin^2\theta \sin^2\phi)].\tag{7}$$

Here R is the photon production rate per unit four-volume in the rest frame of the hot matter, and v is the transverse velocity of the matter in the cell characterized by proper time τ, space-time rapidity η, and radial position r (measured in the frame moving with transverse velocity zero and longitudinal velocity $\tanh\eta$ in the lab). Evaluating the integrals over η and p with the δ functions, we obtain

$$\frac{d^2 N_\gamma}{p_T \, dp_T \, dy}\bigg|_{y=0} = \int d\tau \, \tau \int dr \, 2\pi r \int_0^\pi d\theta \, \sin\theta \int_0^{2\pi} d\phi \, \frac{p_*^3}{p_T^2} \left(\frac{dR}{d^3 p}\right)_{p=p_*}, \tag{8}$$

$$p_* = \frac{p_T}{\gamma \left[\sin^2\theta + 2v\sin\theta\cos\phi + v^2\left(1 - \sin^2\theta\sin^2\phi\right)\right]^{1/2}}. \tag{9}$$

The photon production rate from thermally and chemically equilibrated quark gluon plasma is [12]

$$\frac{dR}{d^3 p} = \frac{5\,\alpha\,\alpha_s}{18\,\pi^2\,p}\,T^2\,e^{-p/T}\,\ln\left(\frac{2.912\,p}{g^2\,T} + 1\right), \tag{10}$$

where $\alpha = 1/137$ and $\alpha_s = g^2/4\pi = 0.4$. (We use the semiempirical formula of Ref. [12], which is almost identical to the exact rate.)

Equation (10) is first order in α_s (or g^2), and as g is of order unity, its accuracy is of the order of unity. We also use it for the hadron gas, as its uncertainty is larger than the difference between the first-order QGP and hadron gas production rates [13]. The contribution of the a_1 resonance as an intermediate state was discussed recently by several authors [14,15,2]. Here we include the contribution of the a_1 meson as parametrized in Ref. [14].

The calculation follows the space-time evolution of the collision based on Eq. (8) and results in nearly exponential spectra. We then mimic the experimental procedure and extract a temperature (the fit temperature T_{fit}) from the obtained spectra. For fitting purposes, we take (8) with $v = 0$ (i.e., ignoring transverse expansion), resulting in the formula [3]

$$\frac{d^2 N}{p_T \, dp_T \, dy} \sim \frac{T^{5/2}}{p_T^{1/2}}\,e^{-p_T/T}\,\ln\left(\frac{2.912\,p_T}{g^2 T} + 1.12\right), \tag{11}$$

which is accurate to about 1% for the range we consider here.

The photon production in the QGP is dominated by quark-gluon collisions. To simulate scenarios where the quark number is smaller than the equilibrium value, we multiply the rate (10) by x, the fraction of the equilibrium number of quarks, for the QGP component of the fluid. This representation of the deviations from chemical equilibrium is valid whenever the quarks and antiquarks are non-degenerate, so that Maxwell-Boltzmann statistics can be used in place of Fermi statistics, and when the production from quark-antiquark annihilation (which is proportional to x^2) is small.

IV. RESULTS

Our standard calculation uses $\tau_0 = 0.2$ fm/c, $x=1$, freeze-out temperature $T_{\text{fo}} = 100$ MeV, and includes the a_1 resonance; if a different value of one of the parameters is given, it is to be assumed that the others are held at the standard values. In Fig. 1, we vary T_c from 150 to 200 MeV and calculate the resulting values of the temperature T_{fit} needed in Eq. (11) to fit the resulting

spectrum for a central S+Au collision at SPS energy. Our standard value for the equilibration time, $\tau_0 = 0.2$ fm/c, implies an initial temperature of $T_0 = 355$ MeV for the S+Au system.

In the absence of transverse expansion, T_{fit} is a monotonically increasing function of T_c, so one can infer T_c given T_{fit} from the measured photon spectrum [3]. This can be seen in the lowest curve, where we have run our simulation without transverse expansion.

Including transverse expansion, we find that we can no longer infer T_c from T_{fit}, due to the nonmonotonicity of the relation (except for long thermalization times; see the curve with $\tau_0 = 1.0$ fm/c, corresponding to $T_0 = 208$ MeV). This demonstrates the large effect of the transverse motion of the fluid on the photon spectrum: lowering T_c decreases the bag constant, which increases the ratio P/e in the QGP, producing more transverse motion. The increase in p_T caused by the fluid motion is enough to overcome the decrease of T_{fit} with decreasing T_c found without transverse expansion. This non-monotonicity occurred for all parameter sets we tried, although for some (e.g., $\tau_0 = 1$ fm/c) the minimum appears outside the range of T_c investigated here. As the initial temperature is lowered, the value of T_c below which the effects of flow dominate also decreases. This may be attributed to the fact that, as T_0 approaches T_c, less flow develops before the mixed phase is reached.
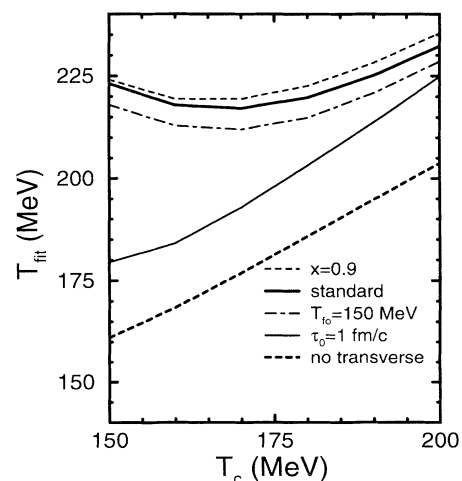

FIG. 1. T_{fit} vs T_c for central S+Au collisions at SPS energy with various parameter sets. The standard set consists of $\tau_0 = 0.2$ fm/c (corresponding to $T_0 = 355$ MeV), $x=1$, $T_{\text{fo}} = 100$ MeV, and includes the a_1 resonance; the other sets differ from the standard one in the value of the parameter indicated.

Contrary to experience without transverse expansion [3], increasing $T_{\rm fo}$ to 150 MeV decreases $T_{\rm fit}$, another indication that the transverse motion has a large effect on the spectrum. Apparently the lower-temperature hadronic matter expands outward at a velocity high enough that the contribution to p_T from this motion more than makes up for the low temperature. Thus removing the contribution from the late stages (by raising $T_{\rm fo}$) decreases $T_{\rm fit}$.

For $x \neq 1$, the quantity we call T_c on the figure is the chemical equilibrium $(x = 1)$ transition temperature,

$$T_c = \left(\frac{90}{34\pi^2}B\right)^{1/4}, \tag{12}$$

rather than the larger nonequilibrium transition temperature used in the simulation, which is given by Eq. (5). We do this because the equilibrium transition temperature is more useful for comparisons with theoretical calculations. The curve for $x = 0.9$ shows that $T_{\rm fit}$ is about 3 MeV higher than for $x = 1$. The increase occurs because the temperature of the mixed phase, which makes a large contribution to the photon spectrum, is raised when x is lowered. We do not show results for other values of x; the change in $T_{\rm fit}$ is approximately linear in x.

The effect of increasing τ_0 to 1 fm/c is dramatic: $T_{\rm fit}$ becomes monotonic within the range of interest, and is lower than for the other parameter sets considered. As mentioned above, this is due to the decrease in the role of the transverse expansion, which is assumed to start at τ_0.

Figure 2 displays the effect of varying the parameters on the spectra, keeping the value of the critical temperature fixed $(T_c = 170$ MeV$)$. We plot $d^2N_\gamma/p_T dp_T dy$ vs p_T for different scenarios. The spectra are nearly exponential. It is seen that increasing the equilibration time (i.e., decreasing the initial temperature) decreases the high p_T contribution to the photon spectrum and thus decreases the fit temperature. Increasing the freezeout temperature removes a fraction of the radiated photons and decreases the yield, also as expected. Excluding the a_1 resonance
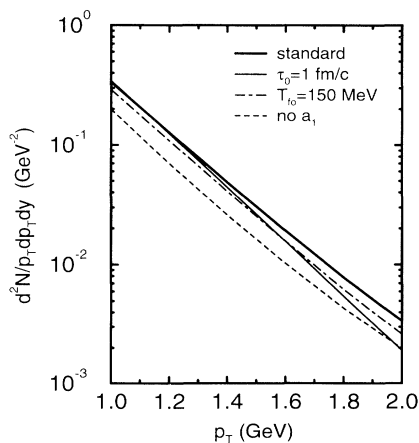
decreases the yield by about one-third in the transverse-momentum range investigated. This is roughly consistent with several other calculations [14–16,2].

Figure 3 shows $d^2N_\gamma/p_T dp_T dy$ vs p_T (per central collision) for the preliminary WA80 data (assuming a minimum bias cross section of 3600 mb), along with calculated spectra using selected parameter sets. The data between 1 and 2 GeV are best fitted with $T_{\rm fit} = 213$ MeV, using Eq. (11). We use this value of $T_{\rm fit}$ and Fig. 1 to extract the value of T_c (between 150 and 200 MeV) for each parameter set. The experimentally determined fit temperature, $T_{\rm fit} = 213$ MeV, is below the values predicted by the model for some parameter choices. In these cases T_c was estimated by minimizing $T_{\rm fit}$.

For the standard parameter set and for $x = 0.9$ we used $T_c=170$ MeV. Note, however, that for $x \neq 1$, the nonequilibrium transition temperature is larger than this, as explained earlier. The difference is sufficient to counteract the decrease in the number of degrees of freedom in the plasma, leading to a somewhat higher yield than with the standard parameters. Due to the large error bars of the preliminary WA80 data, the calculated spectra are consistent with the data points, although generally below them for these parameters. In the absence of transverse expansion, photon production is increased by approximately a factor of 2 by including pion masses [3], so agreement with the preliminary WA80 data will probably be further improved with a more realistic equation of state.

Increasing the equilibration time to $\tau_0=1$ fm/c (and accordingly decreasing the initial temperature) leads to $T_c=190$ MeV. The increase in T_c increases the photon yield. In addition, the lower initial temperature and the higher critical temperature result in less flow being built up by the time the system reaches the mixed phase than with the standard parameter set. Therefore the system spends a longer time in the mixed phase for this set of parameters. This also increases the yield, as pointed out by Shuryak and Xiong [16]. To quantify the difference between these scenarios, we "measured" (in the code) the
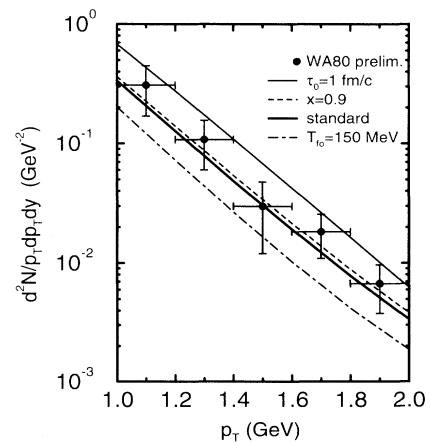

FIG. 2. Photon spectra with different parameter sets keeping $T_c = 170$ MeV constant. The standard set is the same as in Fig. 1.

FIG. 3. The preliminary WA80 data [1] and selected fits. For each curve the value of T_c giving $T_{\rm fit} =213$ MeV from Fig. 1 is used as explained in the text.

total four-volume associated with the mixed phase and found it to be about 25% larger for $\tau_0=1$ fm/c than for $\tau_0=0.2$ fm/c. Our results with the long equilibration time ($\tau_0=1$ fm/c) tend to overestimate the data. Excess photons come from both the QGP and the hadronic phases in our calculation relative to Ref. [16].

Increasing the freeze-out temperature to $T_{\text{fo}}=150$ MeV decreases the photon yield partly because a contribution is removed, and partly because we use $T_c = 160$ MeV (rather than 170 MeV) in this case. Note that 160 MeV$\leq T_c \leq 170$ MeV all give approximately the same T_{fit} for $T_{\text{fo}}=150$ MeV, though the photon spectrum has a larger magnitude when T_c is increased due to the large contribution from the mixed phase. Thus, even if T_c cannot be determined by T_{fit} alone, it may be possible to ascertain T_c by comparing to the total production rate as well.

Figure 4 displays predicted spectra for a central Pb+Pb collision at SPS energy, using the parameter sets from Fig. 3. The initial temperatures corresponding to $\tau_0= 0.2$ fm/c and $\tau_0= 1$ fm/c are $T_0 = 441$ MeV and $T_0 =258$ MeV, respectively. The shapes of the spectra and the relative production rates are similar to those for the S+Au collisions. For comparison, we also show the spectrum obtained in the absence of transverse expansion, taking $T_c = 200$ MeV. We find that transverse expansion has a large effect on the production rate, in apparent disagreement with Ref. [2].

Our conclusion is that transverse expansion destroys the correlation suggested in Ref. [3], so that T_c cannot be determined just from measurements of the shape of the single photon spectrum, as parametrized by T_{fit}. The monotonic dependence of T_{fit} on T_c is destroyed because the transverse flow increases as T_c decreases. However, the total production rate is also sensitive to T_c, so it is
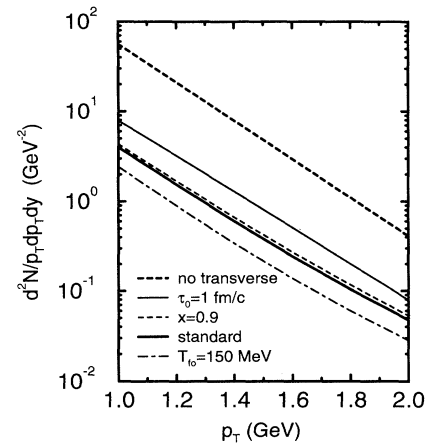

FIG. 4. Predicted photon spectra for central Pb+Pb collisions at SPS energy.

possible that comparison to the production rate instead of just the shape of the transverse momentum spectrum may be sufficient to determine T_c from data. In the transverse-momentum range studied, the inclusion of the a_1 resonance increases the photon yields by about 50%. Preliminary WA80 data appear to rule out large values for the equilibration time.

ACKNOWLEDGMENTS

[1] R. Santo et al., in Proceedings Quark Matter '93, edited by E. Stenlund, H.-Å Gustafsson, A. Oskarsson, and I. Otterlund [Nucl. Phys. A566, 61c (1994)].

[2] D.K. Srivastava and B. Sinha, Phys. Rev. Lett. 73, 2421 (1994).

[3] D. Seibert, Z. Phys. C 58, 307 (1993).

[4] D. Seibert, Phys. Rev. Lett. 68, 1476 (1992); D. Seibert, V.K. Mishra, and G. Fai, Phys. Rev. C 46, 330 (1992).

[5] M. Asakawa and C.M. Ko, Phys. Lett. B 322, 33 (1994); C.M. Ko and M. Asakawa, Nucl. Phys. A566, 447c (1994).

[6] C.M. Ko and D. Seibert, Phys. Rev. C 49, 2198 (1994).

[7] J.D. Bjorken, Phys. Rev. D 27, 140 (1983).

[8] J.-P. Blaizot and J.-Y. Ollitrault, Nucl. Phys. A458, 745

(1986).

[9] E. Shuryak, Phys. Rev. Lett. 68, 3270 (1992).

[10] K. Geiger and J.I. Kapusta, Phys. Rev. D 47, 4905 (1993).

[11] D. Seibert, Phys. Rev. Lett. 67, 12 (1991).

[12] J. Kapusta, P. Lichard, and D. Seibert, Phys. Rev. D 44, 2774 (1991).

[13] H. Nadeau, J. Kapusta, and P. Lichard, Phys. Rev. C 45, 3034 (1992).

[14] L. Xiong, E. Shuryak, and G.E. Brown, Phys. Rev. D 46, 3798 (1992).

[15] C. Song, Phys. Rev. C 47, 2861 (1993).

[16] E. Shuryak and L. Xiong, Phys. Lett. B 333, 316 (1994).